AUTHOR QUERY FORM

Dear Author,

Below are the queries associated with your article; please answer all of these queries before sending the proof back to AIP. Please indicate the following:

Figures that are to appear as color online only (i.e., Figs. 1, 2, 3) _____ All Figures _____ (this is a free service).
Figures that are to appear as color online and color in print _____ None _____ (a fee of \$650 for the first figure and \$325 for each additional figure will apply).

Article checklist: In order to ensure greater accuracy, please check the following and make all necessary corrections before returning your proof.

1. Is the title of your article accurate and spelled correctly? ✓
2. Please check affiliations including spelling, completeness, and correct linking to authors. ✓
3. Did you remember to include acknowledgment of funding, if required, and is it accurate? ✓

Location in article	Query / Remark: click on the Q link to navigate to the appropriate spot in the proof. There, insert your comments as a PDF annotation.
AQ1	Please check that the author names are in the proper order and spelled correctly. Also, please ensure that each author's given and surnames have been correctly identified (given names are highlighted in red and surnames appear in blue).
AQ2	Please provide page range for Ref. 4.
AQ3	Please provide volume number for Ref. 22.
AQ4	Please provide DOI for Refs. 24 and 30.

✓

Thank you for your assistance.

A simple experimental system to illustrate the nonlinear properties of a linear chain under compression

Denis Weaire and Ali Irannezhad
School of Physics, Trinity College Dublin, Dublin 2, Ireland

Adil Mughal
Department of Mathematics, Aberystwyth University, Penglais, Aberystwyth, Ceredigion, Wales SY23, United Kingdom

Stefan Hutzler[a]
School of Physics, Trinity College Dublin, Dublin 2, Ireland

A linear chain of spheres confined by a transverse harmonic potential experiences localized buckling under compression. Here, we present simple experiments using gas bubbles in a liquid-filled tube to demonstrate this phenomenon. Our findings are supported semi-quantitatively by numerical simulations. In particular, we demonstrate the existence of a critical value of compression for the onset of buckling. © *2020 American Association of Physics Teachers.*
https://doi.org/10.1119/10.0000667

I. INTRODUCTION

Linear chains of particles have long been popular in providing simple examples for analysis using classical mechanics. Consequentially, numerous classroom demonstrations entail the study of such chains; examples include the problem of determining the force exerted by a falling chain[1–3] (a long-standing problem, which continues to provoke debate[4]) the vibrations (and normal modes[5]) of a chain of particles,[6] as a means of demonstrating the properties of the catenary[7] (and related curves), the physics of collisions and shock waves,[8] as well as numerous other interesting problems suitable for the undergraduate physics curriculum.[9]

Much of this work has been largely confined to linear elastic theory and dynamics.[5,10] The pedagogical value of such models lies in their essentially one-dimensional nature, which is helpful for observation, analysis, and theory. In many respects, they share the properties of two- and three-dimensional systems and therefore provide an easy introduction to these.

Here, we extend the suite of classroom demonstrations to linear chains of mutually repelling particles. The particles are compressed along the length of the chain (corresponding to being trapped by an axial potential in the related physical systems mentioned below), while also being confined in the radial (or transverse) direction by a cylindrically symmetric potential. We will focus on the case of static equilibrium, for compressions large enough to induce complex nonlinear properties.

Our demonstration experiments and the accompanying theory and simulations are connected with ongoing research in a number of areas, where they may serve as illustration of the underlying physics, but can also offer inspiration for further measurements. Relevant research includes that on laser-cooled ions in Penning traps[11] and dusty plasmas.[12] Related structures have also been observed in experiments with colloids,[13] microfluidic crystals,[14] and magnetic particles.[15] A more accessible system was introduced in Ref. 16, using buoyant plastic spheres in a water-filled tube, rotated by a lathe; structures for a wide range of compression were reported and were further analyzed theoretically in Ref. 17.

The type of arrangement formed by the particles depends on the competition between radial and axial confinement. When radial confinement dominates, the particles form a straight linear chain; however, on reducing the radial force, the preferred (minimum energy) state of the system transitions from a linear chain to a modulated zigzag structure.[18] Such systems have many interesting properties, including buckling, localization (sometimes described in terms of "kinks" or "solitons"), a variety of alternative (meta)stable structures, topological changes, bifurcation diagrams, and a Peierls-Nabarro potential for transitions between them.[18,19] The buckling of a linear chain has also been found to be relevant to mechanical properties of engineered materials[20] and to active colloidal chains in biology.[21] As mentioned, buckled structures commonly occur in formations of cooled ions in traps; these in turn find a range of advanced applications in spectroscopy, quantum computing, and reaction kinematics (see Ref. 22 for a recent review).

In the present paper, we describe for the first time a very simple experimental set-up that may be used to demonstrate and measure many of the generic nonlinear properties of such a system. It is easily realized with the simplest equipment available in the class-room (test tube with stoppers, aquarium pump, and dish-washing solution) (Fig. 1). The experimental arrangement consists of gas bubbles trapped in a horizontal liquid-filled tube. The bubbles are confined axially by opposing walls (stoppers) at either end of the tube. Compressing the linear chain of bubbles leads to buckling. A further increase in compression generates a sequence of different modulated zigzag structures. These are also related to previous studies of the packings of hard spheres in cylinders.[23]

This new type of experiment will enable many fine details to be explored, which have not so far been analysed for any of the more sophisticated systems mentioned above, especially when combined with the numerical simulations of the kind presented here.

II. EXPERIMENTAL METHOD AND RESULTS

Bubbles of equal size are produced by blowing air through a nozzle into a solution of commercial detergent
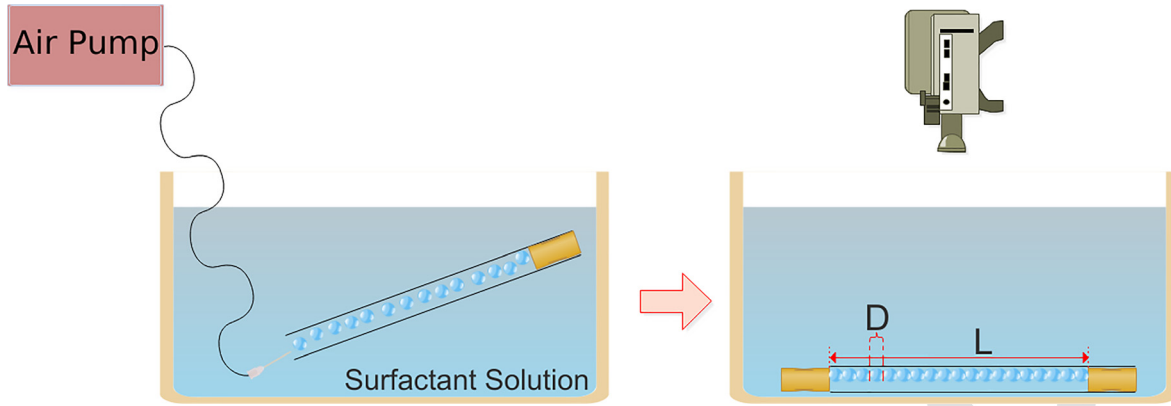
Fig. 1. Sketch of the experimental setup and procedure. After filling, the tube is tilted to release any excess bubbles, so that only a single line of bubbles remains. The second stopper is then inserted and manually adjusted to vary the axial compression of the bubble chain. The observation is carried out under water to avoid air entering the tube. (Inner diameter of the tube: 6.7 mm, outer diameter: 8.0 mm, and axial extension of bubbles: $D = 2.3$ mm).

("*Fairy Liquid*") using an air pump with a flow-control valve. The bubbles are introduced into a perspex tube (inner diameter 6.7 mm, outer diameter 8 mm), which is placed horizontally at the bottom of the container filled with the surfactant solution (Fig. 1), and stoppers are inserted. For a certain separation L_0 of these stoppers, N bubbles are only just in contact with one another and the two stoppers. The uncompressed axial extension D of the bubbles is then $D = L_0/N$. In the experiments reported below, we have used $N = 19$ bubbles with $D = 2.3$ mm.

Decreasing the length of confinement L by manually pushing the stoppers, we may observe and record (as photos or videos) the structures that are formed; for an example, see Fig. 2. For small values of compression Δ, defined as $\Delta = N - L/D$, the chain of bubbles remains straight, with all bubbles suffering equal deformation. However, at some critical value of compression Δ, buckling occurs (see Fig. 2). The critical value of Δ is *zero* for hard spheres and finite for soft (elastic) spheres, as in the case of bubbles.

In this regime, the buckled structures are found to be *planar* for rotating cylinders.[16,17] They are *approximately* so

for the technique here introduced. Further examples are shown in Fig. 3 and numbered for later reference.

To characterize these structures under compression in a simple way, we have determined the width W of the minimal rectangular box, which contains all the bubbles of a particular chain; for an example, see Fig. 4 (top). This is a convenient parameter for measurements by hand from photographs. However, the data reported below were obtained using the image processing software IMAGEJ.[24]

Figure 4 shows the rescaled width W/D for ten different values of compression Δ, for all the structures shown in Fig. 3. The width increases strongly once the compression exceeds its critical value.

Before describing the data in detail, we will comment on a particular feature of the experimental set-up. In the case of an uncompressed chain ($\Delta = 0$) of *hard* spheres the width W is simply D (which in this case coincides with the sphere diameter). However, two effects play a role when interpreting W in our experiments with bubbles. First, optical distortion arising from using liquid-filled tubes leads to a small increase in the ratio W/D, also in the case of hard spheres for these experiments. (We found $W/D \simeq 1.04$ for a chain of *hard* plastic
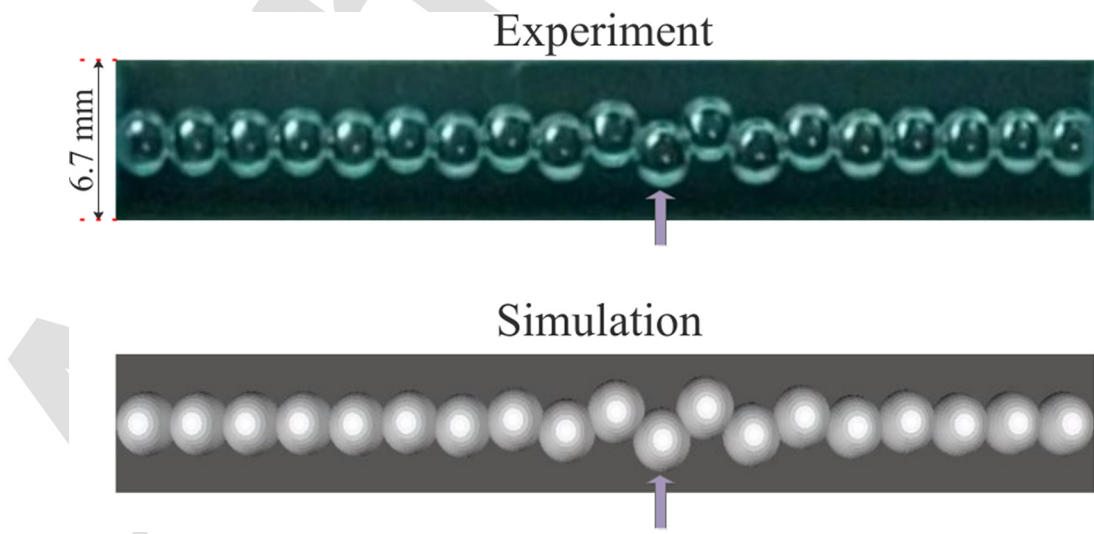

Fig. 2. The compression of a linear chain of bubbles results in buckling, once a critical value of compression is exceeded. (a) Photograph of 19 gas bubbles in a tube filled with surfactant solution for compression $\Delta = 2.36$ (corresponding to image/datapoint 6 in Figs. 3 and 4). (b) A computer simulation of 19 soft spheres using the model of Sec. III and ratio of force constants $k = 2.25$ yields a closely similar structure, cf. the region around the maximally displaced bubble, marked by an arrow.
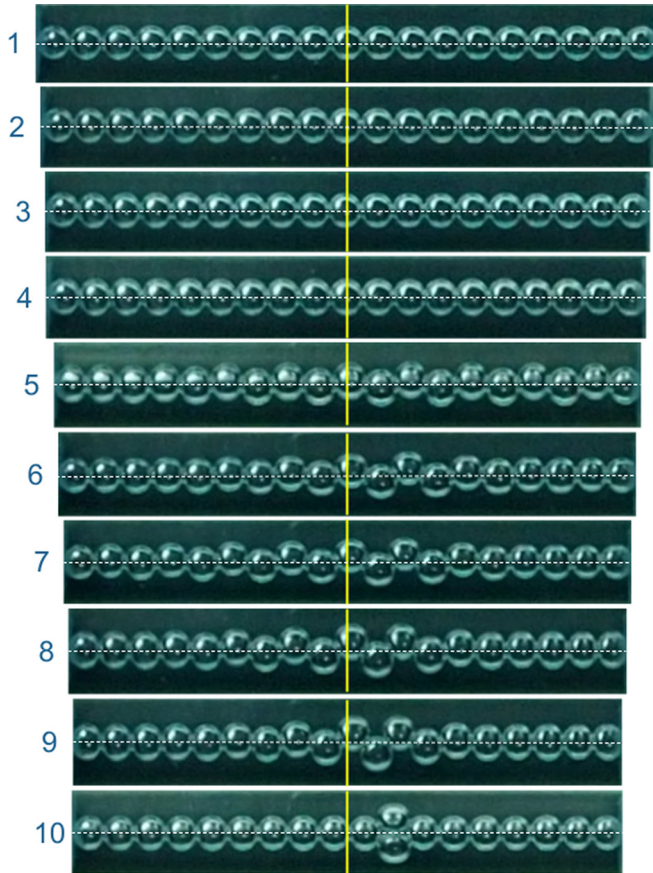
Fig. 3. Sequence of 10 photographs of a chain of 19 bubbles under compression ($\Delta_i = 0.13$, 0.32, 1.00, 1.56, 2.13, 2.36, 2.56, 2.62, 2.80, 2.85). For geometrical dimensions, see the text. Compression was progressively increased by small amounts. The solid yellow line marks the center of each chain. Buckling becomes visible at the fifth image, leading to a modulated zig-zag pattern of bubble displacement. Note eventual exceptional case 10, in which a transverse pair (or *doublet*) of bubbles is surrounded by a straight linear chain. Variation of the experimental procedure can produce localization at other places in the chain.

spheres of diameter 3 mm, placed in the water-filled tube within the container used for the bubble experiments.) Second, our gas bubbles are not spherical even under zero compression Δ, due to the effect of buoyancy, pressing them against the tube surface.

The combination of these two effects can account for the value of $W/D \simeq 1.14$ found for small compression, $\Delta \simeq 0.13$, see Fig. 4. Upon further compression the width increases slightly to about $W/D \simeq 1.23$ for $\Delta \simeq 1.56$. At $\Delta = 2.13$, the chain has clearly buckled, causing a large increase in the width to about $W/D \simeq 1.41$. A further increase in compression results in a roughly linear increase in W, as the profile of lateral displacement becomes increasingly *localized* (see the photograph in Fig. 4).

At values of compression exceeding $\Delta \simeq 2.7$, the localized zig-zag structure gives way to a straight chain containing a "doublet," a transverse pair of bubbles.

A linear extrapolation of the width variation of the buckled structures would identify the onset of buckling at around $\Delta_c \simeq 1.75$. However, buckling is generally associated with a square-root scaling in compression, visible in the simulations described in Sec. III. Taking this into account, we estimate the critical value of compression to lie somewhere in the range $1.8 < \Delta_c < 2.0$ (Fig. 4).
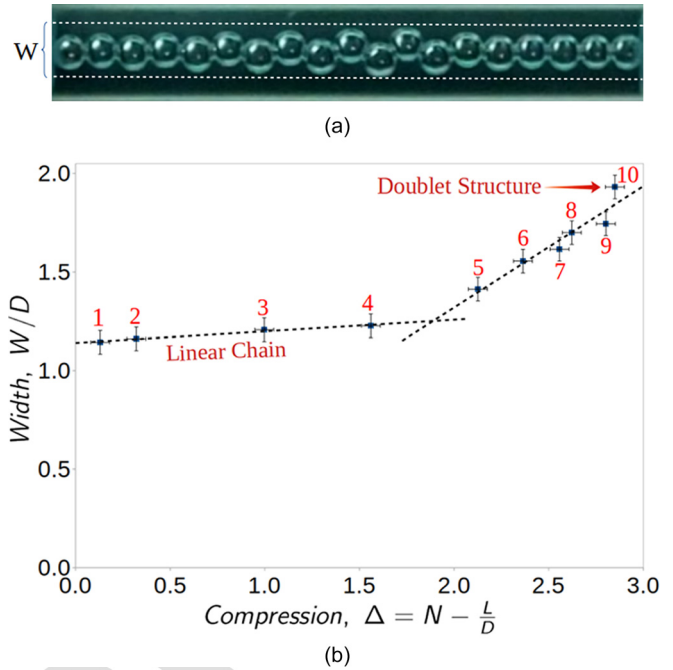

(a)

(b)

Fig. 4. The variation of the normalized chain width W/D with compression Δ reveals the onset of buckling at a critical value of $\Delta_c \simeq 1.9$. Values of Δ exceeding 2.7 lead to the occurrence of an increasing number of doublets within the same structure. (Numbers refer to the chains shown in Fig. 3, and the photograph at the top marks the width W for structure 7.).

III. THEORY AND SIMULATIONS

We have made a preliminary comparison of the above data with the results from an elementary numerical simulation. The basis for this is explained below. We should emphasize that the simple model for bubble-bubble interactions, which we will employ, is *not* intended to be accurate, and so comparison will not be fully quantitative.

We will be concerned with structures of length L, made up of N idealized spherical particles of diameter D; see Fig. 5. We will restrict our analysis to structures formed under low compression, $\Delta = N - L/D$. We have already shown one simulation result in Fig. 2.

To obtain such numerical results, we have used the Durian Model.[25,26] This represents bubbles as spheres whose overlap is associated with a repulsive force between the bubble centres. (A similar approach was suggested earlier.[27]) For a pair of bubbles of equal size, the interaction energy E_i is $E_i = k_1/2(|\vec{R}_i - \vec{R}_{i+1}| - D)^2$, where $\vec{R}_i$ are sphere centres and k_1 is the spring constant for bubble-bubble interaction. The crude model has proved to be useful in foam physics[28,29] in providing qualitative and semi-quantitative insights.

In the present case, we write the total energy due to *contacts*, including the contribution of the two bubbles in contact with the confining walls ($i = 1$) and ($i = N$), in the approximate form,

$$E_{contact} = \frac{k_1}{2} \left[\sum_{i=1}^{N-1} (((X_i - X_{i+1})^2 + (Y_i - Y_{i+1})^2)^{1/2} - D)^2 + \left(\frac{D}{2} - X_1\right)^2 + \left(\frac{D}{2} + X_N - L\right)^2 \right]. \quad (1)$$
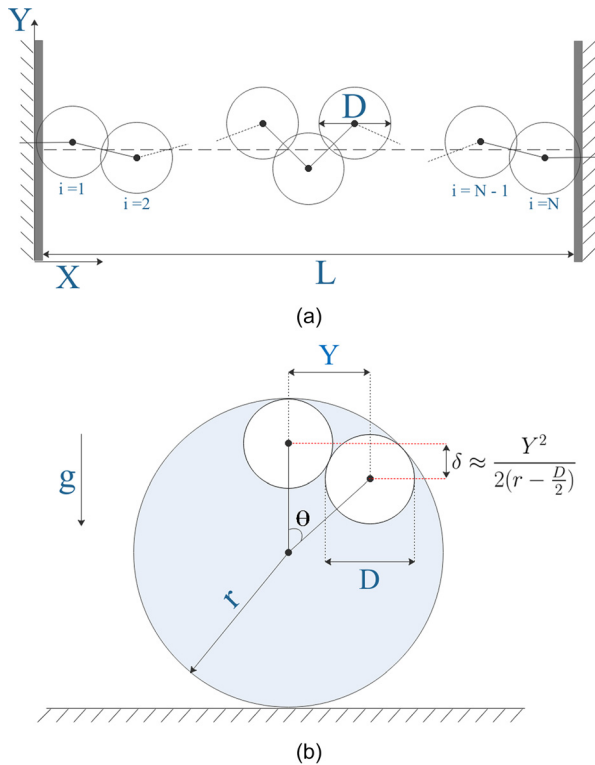
Fig. 5. Schematics for the modeling of a chain of soft spheres under compression. (a) Top view and notation. (b) View along the X direction, showing bubbles (diameter D) pressed against the surface of a liquid filled tube (radius r). For small displacements Y of a bubble in the horizontal direction, its downward movement leads to an increase in potential energy due to buoyancy of approximately $\frac{1}{2}\frac{\Delta\rho g V}{(r-D/2)}Y^2$. Here, $\Delta\rho$ is the density difference and V is the volume of the bubble, $V=\frac{4}{3}\pi(\frac{D}{2})^3$.

190 Only the coordinates X_i and Y_i enter, an approximation
191 that makes the system planar and is valid for small values of
192 compression.
193 The corresponding approximation for the gravitational
194 potential energy due to the *buoyancy* of a particle held in
195 place by the cylindrical surface is

$$E_{gravity} = \frac{k_2}{2}\sum_{i=1}^{N} Y_i^2. \tag{2}$$

196 The force constant k_2 is given by

$$k_2 = \Delta\rho g\,\frac{4}{3}\pi(D/2)^3/(r-D/2), \tag{3}$$

197 where $\Delta\rho$ is the density difference of gas and liquid, g is the
198 acceleration due to gravity, and r is the radius of the cylin-
199 der, see Fig. 5(b).
200 The total energy is thus approximated by $E_{total} = E_{contact}$
201 $+ E_{gravity}$. Expressed as a dimensionless energy, $E = E_{total}/$
202 $(k_2 D^2)$, this may be written as

$$E(\Delta) = \frac{1}{2}k\sum_{i=0}^{N}(\delta_{i,i+1}-1)^2 + \frac{1}{2}\sum_{i=1}^{N}y_i^2, \tag{4}$$

203 where we have introduced the dimensionless quantities x_i
204 $= X_i/D$, $y_i = Y_i/D$, $\delta_{i,i+1} = ((x_i-x_{i+1})^2+(y_i-y_{i+1})^2)^{1/2}$

205 (for $0 < i < N$), $\delta_{0,1}=\frac{3}{2}-x_1$, $\delta_{N,N+1}=\frac{3}{2}+x_n-(N-\Delta)$,
206 and the ratio of the two force constants,

$$k = k_1/k_2. \tag{5}$$

This is essentially the same expression used in Ref. 20.
207 The system has been reduced to two dimensions. The situa-
208 tion is rather different in the other physical systems to which
209 we referred in Sec. I, where planar structures are found to
210 arise for only low compressions, but are not imposed by
211 geometry at the outset (as we have done here). That is, planar
212 structures are found in practice and become twisted at higher
213 compression.
214 Starting from a small value of compression Δ, and a
215 straight linear chain, we progressively increase Δ. For each
216 step, the previous equilibrium structure is used as the starting
217 structure for minimization (in accord with the experimental
218 procedure). Energy E, Eq. (4), is minimized numerically
219 with respect to the coordinates x_i and y_i.
220 Below a critical value of compression (which depends on
221 the value for the ratio k of the force constant, Eq. (5)), the
222 minimum energy arrangement corresponds to that of a
223 straight linear chain, but this buckles to form a zig-zag chain
224 at a critical value of compression, as in the experiment. (A
225 small perturbation is necessary to promote the instability.)
226 We performed computations for increments of $\delta\Delta = 0.01$
227 up to compression $\Delta = 3.0$ for various values of k. The
228 results for $k=2.5$ and $N=19$ are collated in Fig. 6, in terms
229 of the dimensionless maximum transverse displacement,
230 $y_{max} = \max(|y_i|)$. We have found this to be a more straight-
231 forward quantity for comparison with experiment, rather
232 than width W, since W is affected by both optical distortion
233 and bubble deformation, as discussed above.
234 For values of compression slightly exceeding $\Delta_c = 1.83$,
235 we find y_{max} to vary as $(\Delta - \Delta_c)^{1/2}$, as is generally the case
236 in buckling transitions. In this range, the envelope of the dis-
237 placement profile is broad (roughly of cosine form).
238 For higher values of Δ, there is increased localization of
239 buckling, as in the example shown in Fig. 2. Finally, there is
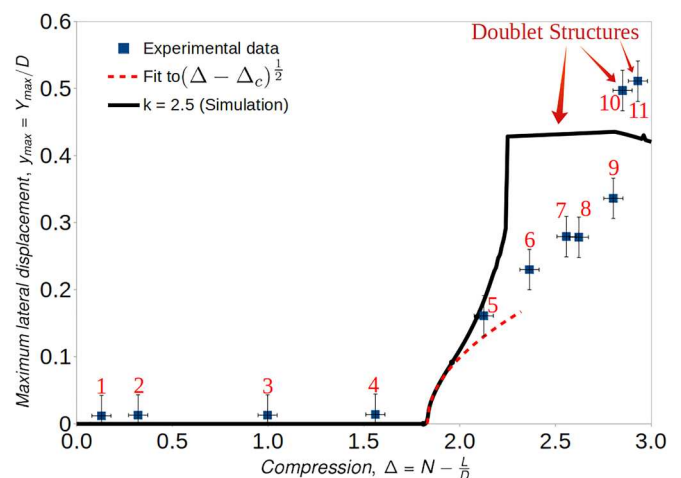240 a sudden jump in the maximum transverse displacement with

Fig. 6. Variation of maximum lateral bubble displacement y_{max} with compression Δ. Data points correspond to the experimental data of Fig. 4. The solid line represents numerical data obtained from a minimization of the energy of a chain of soft particles, Eq. (4), for a value of the force constant ratio $k=2.5$. At the onset of buckling, the numerical results indicate a square-root dependence of y_{max} with compression.

with compression (dashed line).

Fig. 6. Experimental data and results of a model simulation, for the variation of ...

Fig. 7. Buckled chain of 30 steel spheres (diameter 6.32 mm) confined in a perspex cylinder (inner cylinder diameter 1.6 cm) and under compression, $\Delta = 0.85$. The spheres, which are undeformed, are immersed in vegetable oil to reduce friction between them. (The presence of the oil leads to a large optical distortion; the measured ratio of lateral sphere extension to sphere diameter is about 1.9.).

which remain undeformed, ...

increasing compression; at this point, the doublet structure (with a transverse pair of spheres) becomes favourable. The maximum transverse displacement associated with this increases very slightly with compression, before encountering a further transition. Full details of this rich scenario, as well as a comprehensive overview of theory and simulation, are reserved for a future paper.

IV. COMPARISON WITH EXPERIMENT

Figure 6 also presents experimental data for comparison. Here, the maximum lateral bubble displacement $y_{max} = Y_{max}/D$ was obtained by first determining the lateral midpoint of each bubble and then measuring its distance to the tube axis, using the photographs in Fig. 3. (The representation of the buckling of a bubble chain using its width W, as in Fig. 4, might be more suited in the context of a class-room since it requires fewer measurements.)

There is broad agreement between experiment and theory for $k = 2.5$. Increasing k moves the critical value of compression Δ_c towards zero, the value found for the case of hard spheres ($k_1 \rightarrow \infty$).[17] The theory also correctly predicts the occurrence of a doublet structure (number 10 in Fig. 3).

We may also seek to estimate k from the relevant experimental parameters. Setting the dimensional spring constant $k_1 = \gamma/2$,[26] where $\gamma \simeq 0.03$ N/m is the surface tension of our surfactant solution, we can evaluate $k = k_1/k_2$ using Eq. (3). Substituting $\rho = 1000$ kg/m^3, $D = 2.3$ mm, and $r = 3.35$ mm, we obtain $k \simeq 0.5$, i.e., a value of the same order of magnitude as the one found from comparison with numerical data (Fig. 6).

V. FURTHER DEMONSTRATION EXPERIMENTS

The effects of buckling in a chain of particles can also be illustrated using even simpler experimental set-ups.

Figure 7 shows an example of a buckled chain of 30 steel spheres (ball bearings) in a tube, closed with two stoppers. In order to reduce friction, we immersed the spheres in vegetable oil. Related structures can also be investigated using golf or tennis balls in a perspex tube, or even in a section of roof gutter, and doubtless other ingredients await discovery and exploitation.

VI. SUMMARY AND OUTLOOK

We have described a simple experimental set-up, suitable for the class- or lecture room, for the exploration of the nonlinear properties of a chain of spheres under compression. The experiment demonstrates these properties, which have recently led to a number of publications on nano-scale systems.[11,12,30] The simulation method described is straightforward and reproduces key features of the experiment. It might also lend itself to exploration in the context of a computational physics laboratory.

the scaled softness ...

The use of bubbles offers an additional dimension to the experiment, which could be explored: the effective softness of the bubbles is a function of their size. In the present preliminary work, we have used only a single bubble size and treat the softness parameter (constant k in Eq. (4)) as adjustable. Note that k can also be varied by varying the cylinder radius.

In previous work, we analysed the desk-top toy called "Newton's Cradle", i.e., a linear chain of contacting metal balls, suspended from a railing by attached strings, and thus subject to a harmonic confining potential, albeit in the direction of the chain.[31] As is the case in the present work, this system proved to be remarkably rich when analyzed in detail. In particular, the break-up of the line of balls following the initial impact is generally overlooked in physics textbook descriptions. It is hoped that the bubble chain experiment presented here, which shares with the cradle an economy of effort and expense, provides similar stimulation for students to look for non-trivial phenomena in chains of confined spheres.

a)Electronic mail: stefan.hutzler@tcd.ie

[1] M. G. Calkin and R. H. March, "The dynamics of a falling chain: I," Am. J. Phys. **57**(2), 154–157 (1989).

[2] E. Hamm and J. C. Géminard, "The weight of a falling chain, revisited," Am. J. Phys. **78**(8), 828–833 (2010).

[3] J. C. Géminard and L. Vanel, "The motion of a freely falling chain tip: Force measurements," Am. J. Phys. **76**(6), 541–545 (2008).

[4] A. A. Domnyshev, V. A. Kalinichenko, and P. M. Shkapov, "On two experiments with falling chains," J. Phys. Conf. Ser. **1301**(1), ■ p. 012012 (2019).

[5] J. D. Louck, "Exact normal modes of oscillation of a linear chain of identical particles," Am. J. Phys. **30**, 585–590 (1962).

[6] D. Oliver, "Oscillation of a paper-clip chain," Phys. Teach. **34**, 446–447 (1996).

[7] F. Behroozi, P. Mohazzabi, and J. P. McCrickard, "Remarkable shapes of a catenary under the effect of gravity and surface tension," Am. J. Phys. **62**, 1121–1128 (1994).

[8] F. Herrmann and M. Seitz, "How does the ball-chain work?," Am. J. Phys. **50**(11), 977–981 (1982).

[9] G. Péter, G. Honyek, and K. F. Riley, *200 Puzzling Physics Problems: With Hints and Solutions* (Cambridge U.P., Cambridge, 2001), p. 19–20.

[10] M. Reinsch, "Dispersionfree linear chains," Am. J. Phys. **62**, 271–278 (1994).

[11] R. C. Thompson, "Ion coulomb crystals," Contemp. Phys. **56**(1), 63–79 (2015).

[12] A. Melzer, "Zigzag transition of finite dust clusters," Phys. Rev. E **73**(5), 056404 (2006).

[13] A. V. Straube, A. A. Louis, J. Baumgartl, C. Bechinger, and R. P. A. Dullens, "Pattern formation in colloidal explosions," EPL **94**(4), 48008 (2011).

[14]T. Beatus, T. Tlusty, and R. Bar-Ziv, "Phonons in a one-dimensional microfluidic crystal," Nat. Phys. **2**(11), 743 (2006).

[15]J. E. Galván-Moya, D. Lucena, W. P. Ferreira, and F. M. Peeters, "Magnetic particles confined in a modulated channel: Structural transitions tunable by tilting a magnetic field," Phys. Rev. E **89**(3), 032309 (2014).

[16]T. Lee, K. Gizynski, and B. A. Grzybowski, "Non-equilibrium self-assembly of monocomponent and multicomponent tubular structures in rotating fluids," Adv. Mater. **29**(47), 1704274 (2017).

[17]J. Winkelmann, A. Mughal, D. Weaire, and S. Hutzler, "Equilibrium configurations of hard spheres in a cylindrical harmonic potential," EPL **127**, 44002 (2019).

[18]H. Landa, B. Reznik, J. Brox, M. Mielenz, and T. Schätz, "Structure, dynamics and bifurcations of discrete solitons in trapped ion crystals," New J. Phys. **15**(9), 093003 (2013).

[19]M. Mielenz, J. Brox, S. Kahra, G. Leschhorn, M. Albert, T. Schätz, H. Landa, and B. Reznik, "Trapping of topological-structural defects in coulomb crystals," Phys. Rev. Lett. **110**(13), 133004 (2013).

[20]R. K. Pal, F. Bonetto, L. Dieci, and M. Ruzzene, "A study of deformation localization in nonlinear elastic square lattices under compression," Philos. Trans. R. Soc. A **376**(2127), 20170140 (2018).

[21]S. Gonzalez and R. Soto, "Active colloidal chains with cilia-and flagella-like motion," New J. Phys. **20**(5), 053014 (2018).

[22]B. R. Heazlewood, "Cold ion chemistry within coulomb crystals," Mol. Phys., 1–8 (2019).

[23]A. Mughal, H. K. Chan, D. Weaire, and S. Hutzler, "Dense packings of spheres in cylinders: Simulations," Phys. Rev. E **85**(5), 051305 (2012).

[24]M. D. Abràmoff, P. J. Magalhães, and S. J. Ram, "Image processing with ImageJ," Biophotonics Int. **11**(7), 36–42 (2004).

[25]D. J. Durian, "Foam mechanics at the bubble scale," Phys. Rev. Lett. **75**, 4780–4783 (1995).

[26]D. J. Durian, "Bubble-scale model of foam mechanics: Melting, nonlinear behavior, and avalanches," Phys. Rev. E **55**, 1739–1751 (1997).

[27]F. Bolton and D. Weaire, "Rigidity loss transition in a disordered 2D froth," Phys. Rev. Lett. **65**, 3449 (1990).

[28]D. Weaire and S. Hutzler, *The Physics of Foams* (Clarendon Press, Oxford, 1999).

[29]I. Cantat, S. Cohen-Addad, F. Elias, F. Graner, R. Höhler, O. Pitois, F. Rouyer, and A. Saint-Jalmes, *Foams: Structure and Dynamics* (Oxford U.P., 2013).

[30]A. V. Chaplik, "Instability of quasi-one-dimensional electron chain and the "string-zigzag" structural transition," JETP Lett. **31**(5), 275–278 (1980).

[31]S. Hutzler, G. Delaney, D. Weaire, and F. MacLeod, "Rocking Newton's cradle," Am. J. Phys. **72**(12), 1508–1516 (2004).

vol 117, p. 1934-1941

AQ3

AQ4

There is not any "doi" for that paper.